Adsorption Study of Acetone on Acid-Doped Ice Surfaces between 203 and 233 K

E. Journet, S. Le Calvé,* and Ph. Mirabel

Centre de Géochimie de la Surface / CNRS and Université Louis Pasteur, 1 rue Blessig, F-67084 Strasbourg Cedex, France

Received: March 24, 2005; In Final Form: May 27, 2005

Adsorption studies of acetone on pure ice surfaces obtained by water freezing or deposition or on frozen ice surfaces doped either with HNO_3 or H_2SO_4 have been performed using a coated wall flow tube coupled to a mass spectrometric detection. The experiments were conducted over the temperature range 203−233 K and freezing solutions containing either H_2SO_4 (0.2 N) or HNO_3 (0.2−3 N). Adsorption of acetone on these ice surfaces was always found to be totally reversible whatever were the experimental conditions. The number of acetone molecules adsorbed per ice surface unit N was conventionally plotted as a function of acetone concentration in the gas phase. For the same conditions, the amount of acetone molecules adsorbed on pure ice obtained by deposition are about 3−4 times higher than those measured on frozen ice films, H_2SO_4-doped ice surfaces lead to results comparable to those obtained on pure ice. On the contrary, N increases largely with increasing concentrations of nitric acid in ice surfaces, up to about 300 times under our experimental conditions and for temperatures ranging between 213 and 233 K. Finally, the results are discussed and used to reestimate the partitioning of acetone between the ice and gas phases in clouds of the upper troposphere.

Introduction

Recent measurements in the upper troposphere (UT) have revealed the presence of oxygenated volatile organic compounds (VOC), such as acetone, that probably play an important role on the ozone cycle in this region. In fact, unexpectedly high acetone concentrations (up to 3000 pptv) have been determined.[1−4] The upper troposphere is characterized by its low temperatures (188−228 K) and by the presence of cirrus clouds which can cover a substantial portion (up to 25%) of the earth's surface.[5,6] At temperatures below 233 K, cirrus clouds are predominantly composed of ice crystals,[7] and these crystals can provide surfaces for trace gas interactions.

The main sources of acetone in the atmosphere are the direct biogenic emissions and its in situ generation by oxidation of isoalkanes and monoterpenes.[3,8] Other minor contributions arise from biomass burning,[9] dead plant matter via abiological processes,[10] and direct anthropogenic emissions. Once in the lower atmosphere, acetone can react with OH radicals or can be photodissociated[11] but can also be eliminated by wet and dry depositions. Its resulting tropospheric lifetime has been estimated of the order of 15 days,[8] a time long enough to allow long-range transportation.

Gierczak et al.[12] have shown that photolysis is the main loss process for acetone in the UT, while the reaction with OH radicals dominates its loss rate near the Earth's surface. The photolysis of acetone leads to an enhanced abundance of HO_X ($HO_X = OH + HO_2$) and of peroxyacetyl nitrate (PAN) in the UT. The production of HO_X can then affect the concentrations of many other trace gases and is likely to modify the ozone cycles in this region while PAN can transport nitrogen oxides from a region of the atmosphere to another.

The uptake of atmospheric pollutants on ice surfaces has been extensively studied for more than 10 years, given their potential impact on the stratospheric ozone hole. Therefore, attention has mainly focused on halogenated or nitrated species such as HCl, HOBr, $ClONO_2$, and HNO_3.[13] In contrast, very few articles have been devoted to the interactions of oxygenated organic compounds with ice and, in this respect, the adsorption of acetone on pure ice is certainly the system that has been studied the most extensively.[14−18] On the basis of the convergence of these experimental works, a relatively clear understanding of the acetone behavior on pure ice surfaces has emerged, in fair agreement with theoretical results.[19,20]

However, pure ice is not representative of the cloud surfaces in the UT since many impurities like HNO_3, or H_2SO_4[21,22] may affect their surface properties. The presence of such impurities can influence the number of adsorbed molecules on the surface or promote heterogeneous reactions and therefore, in both cases, change the partitioning of acetone between the gaseous and the solid phases.

The goal of the present study is to examine the interaction of acetone with ice surfaces doped with either H_2SO_4 or HNO_3, at temperatures relevant for the UT, i.e., from 203 to 233 K and to compare the surface coverages of acetone on these doped ice surfaces with those obtained on pure ice.[18] To our knowledge, adsorption of acetone on several forms of nitric acid-coated ice at temperatures from 190 to 200 K has already been investigated,[17] but this study is the first investigation on sulfuric acid-coated ice surfaces. Note that Hudson et al. did not observe any uptake of acetone on an ice film with a monolayer HNO_3 coverage, on a supercooled 4:1 HNO_3/H_2O solution or on a NAT film.

Our experimental data were then used to reestimate the partitioning of acetone between ice and gas phases in the densest clouds of the upper troposphere.

Experimental Section

The uptake of acetone on ice surfaces was studied using a vertical coated wall flow tube (CWFT) coupled to a mass

* Corresponding author. Fax: +33-(0)3-90-24-04-02. E-mail: slecalve@illite.u-strasbg.fr

10.1021/jp051524u CCC: $30.25
Published on Web 07/06/2005

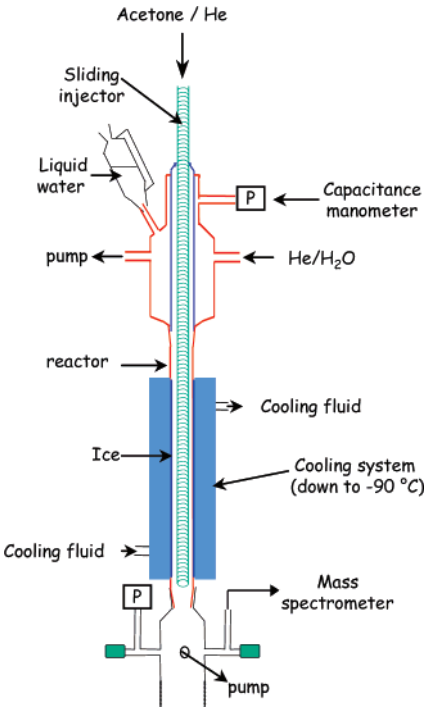

Figure 1. Schematic illustration of the vertical coated wall flow tube.

spectrometer, already described elsewhere.[18] We will therefore provide only a brief summary of its principle operation. The apparatus, which is shown in Figure 1, has a double jacket to allow the system to be operated at low temperature. The cooling fluid was circulated in the inner jacket from a cooler/circulator (Huber, Unistat 385) while vacuum was maintained in the outer jacket for thermal insulation. The temperature of the flow tube could be cooled and regulated between 203 and 233 K.

The jacketed flow tube was approximately 40 cm in length with an internal diameter of 2.8 cm. The ice surface was prepared by totally wetting, with either Milli-Q water (18 MΩ cm) or solutions containing HNO_3 (0.2−3 N) or H_2SO_4 (0.2 N), the inner wall of the flow tube that was precooled between 243 and 263 K depending on the solution. The viscous aqueous film was then cooled to the desired temperature over a period of 10−30 min. The thickness of the ice film was estimated between 50 and 150 μm

In some other experiments, the ice surface has been prepared by direct deposition of water vapor on the inner wall of the flow tube. For this, a large excess of water vapor was introduced through the warming injector that was moved by step of 4 cm every 3−4 min. The obtained ice film was uniform, opaque with a thickness of approximately 80 μm.

For both types of surfaces, the thickness of the ice film was estimated by weighting the resulting liquid water, when the ice film was melted at the end of the experiment.

The helium carrier gas (UHP certified to >99.9995% from Air Liquide) was used without further purification. During the experiment, water vapor was added to the main He flow in order to provide a partial pressure of water, equal to the vapor pressure of water over the ice film, and therefore inhibit net evaporation of the ice film. The resulting humidified helium flow was injected at the upstream end of the flow reactor.

Acetone (99.8%) was purchased from Carlo Erba and was further purified before use by repeated freeze, pump, and thaw cycles as well as by fractional distillation. To perform an experiment, acetone was then premixed with helium in a 10 L glass light-tight bulb to form 1.1×10^{-2} to 5.4×10^{-2} % mixtures, at a total pressure of ≈ 800−950 Torr. The mixture containing acetone was injected into the flow tube reactor via a sliding injector (Figure 1). This later permits one to change the deposition distance which can be varied up to 40 cm in order to change the gas/ice interaction time (0−700 ms) or the exposed ice film surface (120−260 cm^2). The injector was jacketed and a heating tape was wound up in the jacket, to ensure a gentle heating of the injector.[18]

All the gases flowed into the reactor through Teflon tubing. The gas mixture containing acetone and water vapor diluted in helium was flowed through the reactor with a linear velocity ranging between 60 and 120 cm s^{-1}. The concentrations of acetone in the gas phase were calculated from their mass flow rates, temperature and pressure in the flow tube (CWFT). All the flow rates were controlled and measured with calibrated mass flowmeters (Millipore, 2900 series) and the pressure that ranged between 1.9 and 2.5 Torr, was measured with two capacitance manometers (Edwards, 622 Barocel range 0−100 Torr and Keller, PAA-41 range 0−76 Torr) connected at the top and bottom of the flow tube. Under our experimental conditions, the mixing time τ_{mix} between acetone flow and the main He flow was lower than 2 ms[23] which corresponds to a mixing length smaller than 0.3 cm.

The gas stream coming out of the flowtube was analyzed using a differentially pumped mass quadruple spectrometer Pfeiffer Vacuum QMS. Acetone was monitored at the parent ion $CH_3C(O^+)CH_3$ peak at $m/z = 58$ amu or at $m/z = 43$ amu which corresponds to the main fragment ion $CH_3C(O^+)$, using a temporal resolution of 60 ms, an ionization energy of 70 eV and an emission current of 1000 μA.

Results and Discussion

Uptake experiments were performed by first establishing a highly stable flow of acetone in the injector, this injector being positioned past the end of ice film. The injector was then moved quickly to an upstream position so that the ice film is exposed to acetone. The uptake of acetone on the ice film leads to a drop of signal as shown in Figure 2, parts a and b. After a time scale ranging from a few seconds to several minutes, the ice surface was then saturated and the MS signal returned to its initial level. When the injector was pushed back, the acetone desorbed from the ice surface, and the signal increased and then again returned to its initial level. Similar experiments were conducted for various ice surfaces over a temperature range of 213−233 K and for gas-phase concentrations varying from 2.5×10^{11} to 1.0×10^{13} molecules cm^{-3} (see Table 1).

Surface Coverage. The number of acetone molecules adsorbed on the ice surface was determined from the integrated area of the adsorption peak (in molecule s cm^{-3}) and the total flow rate in the flow tube (cm^3 s^{-1}). The surface coverage N (in molecules cm^{-2}) of acetone on ice was then calculated from the exposed ice surface S_{ice} (in cm^{-2}) according to $N = N_{ads}/S_{ice}$ where N_{ads} is the number of acetone molecules adsorbed on the exposed ice surface.

For each kind of ice surfaces, the experiments were performed using different diluted mixtures and several newly generated ice surfaces in order to verify the reproducibility of the data.

The plots of surface coverages N vs the gas-phase concentrations at three studied temperatures (213, 223, and 233 K) and for various ice surfaces are shown in Figures 3−5, respectively. The relative errors on the gas-phase concentrations (horizontal error bars) calculated from the possible uncertainties on each flow, total pressure etc. range between 5 and 25%. The quoted errors on N (vertical error bars) arise from uncertainties made

TABLE 1: Experimental Conditions and Monolayer Capacity Corresponding to Adsorption of Acetone on Ice Surfaces, where the errors bars are given at 2σ levels (see text)

T (K)	ice surfaces	[acetone] (molecule cm^{-3})	N range (molecule cm^{-2})	N_M ($\pm 2\sigma$) (molecule cm^{-2})	ref
213	pure ice	5.4×10^{10} to 1.2×10^{13}	4.2×10^{11} to 5.4×10^{13}	$(1.20 \pm 0.05) \times 10^{14}$ [a]	18
	ice deposition	4.6×10^{11} to $7{,}7 \times 10^{12}$	3.2×10^{13} to 1.1×10^{14}	$(1.5 \pm 0.2) \times 10^{14}$ [a]	this work
	H_2SO_4 0.2 N	5.2×10^{11} to 4.8×10^{12}	5.7×10^{12} to 3.2×10^{13}	$(0.6 \pm 0.1) \times 10^{14}$ [a]	this work
	HNO_3 1N	$2.7 \times 10^{11} - 7{,}4 \times 10^{12}$	2.5×10^{14} to 4.7×10^{15}	n.d.[b]	this work
223	pure ice	5.1×10^{11} to $7{,}6 \times 10^{12}$	1.2×10^{12} to 1.6×10^{13}	$(1.43 \pm 0.13) \times 10^{14}$ [a]	18
	H_2SO_4 0.2 N	5.8×10^{11} to 4.6×10^{12}	1.1×10^{12} to 9.8×10^{12}	$(0.7 \pm 0.1) \times 10^{14}$ [a]	this work
	HNO_3 0.2N	4.4×10^{11} to 9.7×10^{12}	3.9×10^{12} to 2.4×10^{14}	n.d.[b]	this work
	HNO_3 0.5N	4.9×10^{11} to 6.8×10^{12}	1.6×10^{13} to 4.0×10^{14}	n.d.[b]	this work
	HNO_3 1N	2.6×10^{11} to $7{,}6 \times 10^{12}$	6.2×10^{13} to 1.3×10^{15}	n.d.[b]	this work
	HNO_3 3N	2.5×10^{11} to 1.0×10^{13}	1.3×10^{14} to 8.4×10^{15}	n.d.[b]	this work
233	pure ice	4.8×10^{11} to 9.4×10^{12}	4.8×10^{11} to 6.0×10^{12}	n.d.[b]	this work
	HNO_3 0.5N	4.8×10^{11} to 9.1×10^{12}	6.2×10^{12} to 2.3×10^{14}	n.d.[b]	this work
	HNO_3 1N	4.7×10^{11} to 7.3×10^{12}	$4{,}7 \times 10^{13}$ to 4.5×10^{14}	n.d.[b]	this work

[a] These values were obtained from the best fit to the experimental data, using the Langmuir equation, although the asymptote was not yet reached; [b] n.d.: not determined since our experimental data are not satisfactory fitted by a Langmuir isotherm.

on the total flow rate, exposed ice area and concentrations in the gas phase. They also include a systematic error of 2% that corresponds to the error on the integrated area of adsorption peak. These resulting errors on N varie between 7 and 30%.

Isotherms. Both Langmuir and BET isotherm theories have been used to analyze our experimental data. In Langmuir theory, adsorption cannot proceed beyond a monolayer coverage while in the BET model, the initial adsorbed layer can act as a substrate for further adsorption.

Langmuir Isotherm. Assuming only monolayer coverage, the number of molecules adsorbed per area of ice surface depends on the gas-phase concentration of acetone (in molecules cm^{-3}), as shown in the Langmuir expression:

$$\theta = \frac{N}{N_M} = \frac{K_{ads}(T)[\text{acetone}]}{1 + K_{ads}(T)[\text{acetone}]} \quad (1)$$

where θ is the fractional coverage, N_M is the monolayer capacity (in molecules cm^{-2}), and $K_{ads}(T)$ is the temperature-dependent Langmuir constant that describes the partitioning between molecules adsorbed on ice surface and those in the gas phase (cm^3 molecule^{-1}).

BET Isotherms. The most convenient form of the BET equation for application to experimental data is given by the following equation:

$$Y = \frac{p/p_0}{N(1 - (p/p_0))} = \frac{1}{N_M C} + \frac{C - 1}{N_M C} p/p_0 \quad (2)$$

where Y is the BET function,[24] p and p_0 are, respectively, the partial pressure of the compound in the flow tube and its saturation pressure, and C is the BET constant (no unit). Saturation pressures p_0 were calculated from the Antoine equation:

$$\log p_0 = a - \frac{b}{T + c} \quad (3)$$

For acetone, the Antoine parameters available in the literature[25] are $a = 4.424$, $b = 1312.3$, and $c = -32.4$. The resulting saturation vapor pressures of acetone are as follows (in Torr): 1.04 (213 K); 2.59 (223 K); 5.79 (233 K).

Adsorption on Pure Ice Surfaces. Whatever is the type of surface (frozen or deposited), the integrated areas of the adsorption and desorption peaks were found to be the same, within experimental errors, so that adsorption of acetone on ice could be considered reversible. Figure 3 shows the surface coverage for frozen and deposited surfaces at 213 K and for acetone concentrations varying between 4.6×10^{11} and 7.7×10^{12} molecules cm^{-3}. The experimental data were calculated assuming that the ice surface area is equal to the geometric Pyrex area. Our results obtained on deposited ice surfaces are shown in Figure 3 together with those obtained on pure ice with the

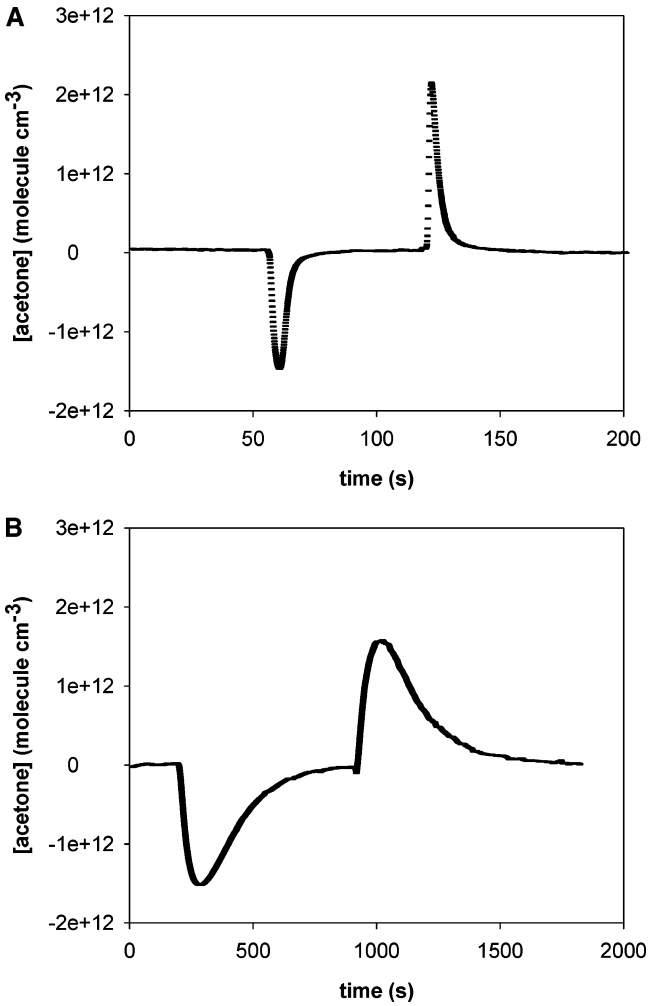

Figure 2. Acetone concentration in the gas phase as a function of time during the adsorption of acetone on ice surfaces for (a) pure ice and (b) ice doped with $HNO_3 = 3$ N at 223 K with [acetone] = 1.5×10^{12} molecules cm^{-3}.

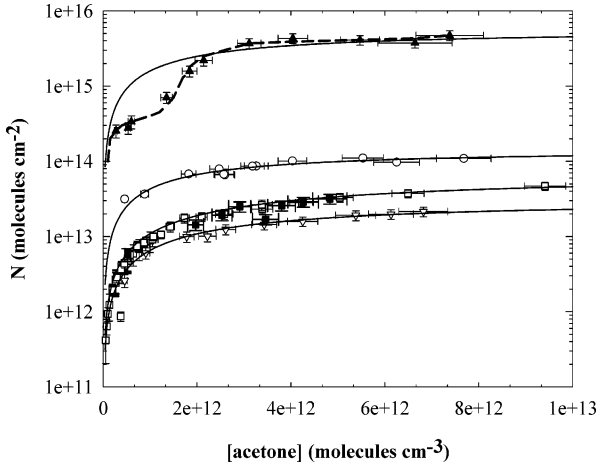

Figure 3. Surface coverage of acetone vs its gas-phase concentration at 213 K on: pure ice obtained by freezing (□),[18] pure ice obtained by deposition from the vapor (○), frozen ice surfaces doped with (■) H_2SO_4, 0.2 N, and (▲) HNO_3, 1 N, before transformation and (▽) HNO_3, 0.2 N, after transformation. The solid lines represent the Langmuir isotherm obtained according to eq 1 while the dashed line fits the experimental data for ice surfaces doped with HNO_3, 3 N.

same technique.[18] Note that few additional experiments were nevertheless performed on frozen pure ice films in this work in order to check if we obtained the same values than Peybernès et al.[18] at 213 K. Our experimental data obtained on deposited ice films were fitted according to Langmuir and BET models in order to derive the monolayer capacity N_M (in units of 10^{14} molecules cm^{-2}): $N_M = 1.4 \pm 0.3$ (BET) and $N_M = 1.5 \pm 0.2$ (Langmuir). These determinations are similar to the average value of $(1.3 \pm 0.3) \times 10^{14}$ molecules cm^{-2} found previously by Peybernès et al.[18] on frozen ice surfaces in the temperature range of 193−223 K. For the same temperature and acetone concentrations in the gas phase, the number of adsorbed molecules on deposited ice surfaces is about 3−4 times higher than that measured on frozen ice films. This reflects the fact that ice surfaces obtained by deposition from the vapor show a dendritic structure which promotes adsorption at a relative low concentration of acetone (isotherm of type I according to Brunauer's classification,[24]). Note that, under our experimental conditions (temperature above 200 K and pressure below 1 atm), the films are necessarily polycrystalline,[26] whatever technique is used to prepare them from pure water.

Adsorption on Ice Surfaces Doped with H_2SO_4. Some experiments were performed on ice films doped with H_2SO_4 (0.2 N) at 213 and 223 K for concentration of acetone ranging between 5.2×10^{11} and 4.8×10^{12} molecules cm^{-3}. Under these conditions, reversible adsorption was always observed for both temperatures and the number of adsorbed molecules on these surfaces was comparable to those already measured on pure ice as shown in Figures 3 and 4. The BET analysis did not allow us to extract N_M values since the plot of Y vs p/p_0 does not give any straight line in the studied range of acetone concentrations. On the contrary, the data are satisfactory fitted with a Langmuir isotherm from which a value of $N_M \sim (6-7) \times 10^{13}$ molecules cm^{-2} is derived for both temperatures. As a conclusion, the presence of sulfuric acid on ice did not enhance the adsorption of acetone, at least under our experimental conditions.

Adsorption on Ice Surfaces Doped with HNO_3. Experiments were conducted on ice films doped with HNO_3 (0.2−3 N) between 203 and 233 K for acetone concentrations varying between 2.5×10^{11} and 1.0×10^{13} molecules cm^{-3}. The adsorption and desorption peaks obtained on these doped ice surfaces are very different from those collected on pure ice, as shown in Figure 2. The adsorption peaks on pure ice extend over a few seconds while they spread out over more than 30 min for ice doped with HNO_3 (3 N). However, adsorption of acetone was always reversible *under our experimental conditions* whatever the concentration of HNO_3. This observation is consistent with the fact that no product has been detected suggesting that no reaction occurred.

In the temperature range 213−233 K, the number of acetone molecules adsorbed on the ice surfaces doped with HNO_3 increased by 1 or 2 orders of magnitude compared to pure ice surfaces and, as can be seen in Figures 3−5, the surface coverage increases with the nitric acid concentration (which varied between 0.2 and 3 N). Furthermore, the shapes of the curves are changed (see for example the upper curve in Figure 3) and show a behavior similar to type IV isotherms of Brunauer's classification, characteristic of mesoporous material.

At 223 K for example, and for an acetone concentration of 7.5×10^{12} molecules cm^3 in the gas phase, the number of adsorbed molecules are as follows: $N \sim 2 \times 10^{13}$ (pure ice);

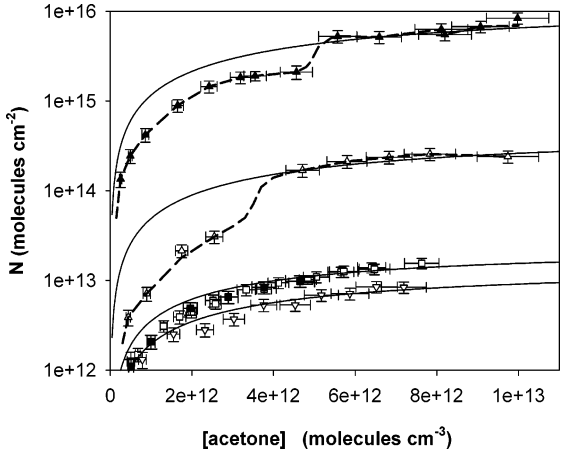

Figure 4. Surface coverage of acetone vs its gas-phase concentration at 223 K for frozen pure ice (□),[18] and ice surfaces doped with (■) H_2SO_4, 0.2 N, (△) HNO_3, 0.2 N before transformation, (▲) HNO_3, 3 N before transformation, and (▽) HNO_3, 0.2 N after transformation. The solid lines represent the Langmuir isotherm obtained according to eq 1 while the dashed lines fit the experimental data for ice surfaces doped with HNO_3, 0.2 and 3 N.

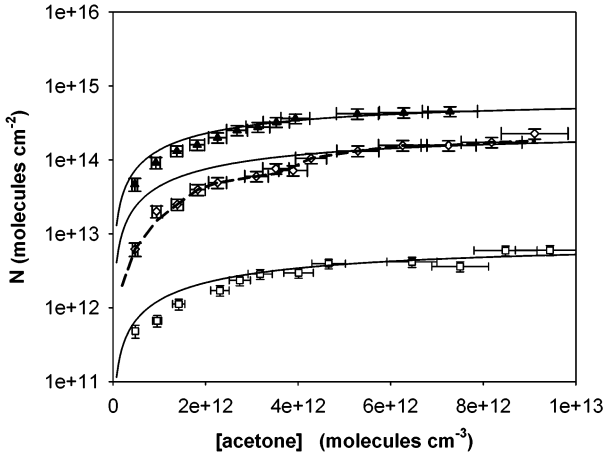

Figure 5. Surface coverage of acetone vs its gas-phase concentration at 233 K for frozen pure ice (□), and ice surfaces doped with either (◇) HNO_3, 0.5 N, before transformation or (▲) HNO_3, 1 N, before transformation. The solid lines represent the Langmuir isotherm obtained according to eq 1 while the dashed line fits the experimental data for ice surfaces doped with HNO_3 0.5 N.

Figure 6. Digital pictures (a) before the ice transformation, (b) during the ice transformation, and (c) after the ice transformation, for a freezing solution of HNO_3, 1 N, at 203 K. Note that the stripes correspond to the winding of the resistance around the warming and sliding injector (in white).

$N \sim 3 \times 10^{14}$ (HNO_3 0.2 N); $N \sim 5 \times 10^{14}$ (HNO_3 0.5 N); $N \sim 1 \times 10^{15}$ (HNO_3 1 N); $N \sim 6 \times 10^{15}$ (HNO_3 3 N) i.e., with a 3 N acid concentration, the number of adsorbed molecules is 300 times more important than on pure ice. Even at the lowest HNO_3 concentration i.e., $[HNO_3] = 0.2$ N, the amount of adsorbed molecules is 1 order of magnitude higher than that determined on pure ice. Similar behavior can be observed at either 213 or 233 K.

Because of the shape of the curves, neither BET or Langmuir theories can be used to successfully fit the S-shaped experimental data on HNO_3 doped-ice, in the studied range of acetone concentrations. Either at 213 K for ice surfaces doped with HNO_3 1 N (before transformation) or at 223 K for ice surfaces doped with HNO_3 0.2 N and 3 N (before transformation), the isotherms clearly exhibit a large "jump" at acetone concentrations of about 1.6×10^{12} molecules cm^{-3} (HNO_3 1 N) at 213 K, 3.6×10^{12} (HNO_3 0.2 N) and 5×10^{12} (HNO_3 3 N) molecules cm^{-3} at 223 K, respectively. To these values correspond the following vapor pressure ratios p/p_o : 0.045 at 213 K, 0.043 (HNO_3 0.2 N) and 0.061 (HNO_3 3 N) at 223 K. According to these values, the "jump" at 233 K is expected at approximately the same ratios which correspond to $(8-11) \times 10^{12}$ molecules cm^{-3}, i.e., at the limit of our experimental acetone concentrations and well above the concentrations found in the atmosphere.

During these experiments, it was observed that, in some cases, the ice film, which originally was transparent, became opaque (see Figure 6). This happened when the ice film, exposed to acetone vapor, was cooled to temperatures slightly below 213 K (in the range 210−200 K). This opacity, which was not observed in our previous work with pure ice[18,27,28] remained when the ice was reheated to the normal operating conditions i.e., for temperatures in the range 213−233 K. Therefore, a systematic study of acetone adsorption was made on these opaque films at temperatures varying between 203 and 223 K. It appears that the number of acetone molecules adsorbed on these opaque ice surfaces is comparable (or slightly lower) to those obtained on pure frozen ice films (lower curves in Figures 3 and 4). At 203 K and for opaque ice surfaces doped with HNO_3 1 N, the number of adsorbed acetone molecules was approximately two times lower than that measured on pure ice films. This means that the macroscopic change observed visually for temperatures slightly below 213 K was probably accompanied by microscopic modifications of the surface of the film.

The phase diagram of the HNO_3-H_2O mixture does not show any phase transformation for temperatures below 231 K, at least for the acid concentrations used in the present work.[29] Such transformation was not observed in our previous study made on pure ice for temperatures in the range 193−223 K.[18,27] Therefore, it is possible that this transformation reflects the influence of acetone on the surface structure of the ice doped with HNO_3.

If many studies have been reported on the adsorption of acetone on pure ice,[16−18,30,31] only one has been focused on its adsorption on ice doped with HNO_3.[17] Hudson et al. have investigated, using a Knudsen cell, the interaction of several volatile organic compounds including acetone, with nitric acid doped ice at temperatures from 190 to 200 K. Studies on nitric acid trihydrate (NAT), on ice with monolayer coverage of HNO_3 and on a supercooled HNO_3/H_2O solution showed no measurable uptake in this temperature range. However, these results are not in contradiction with ours since they were obtained for a different temperature range and with HNO_3 doped ice surfaces prepared in very different ways. In our experiments, when the temperature of the ice film is allowed to go below 210 K, very small uptakes are measured either at 203 K or when the temperature is raised to 213−223 K after modification of ice.

Atmospheric Implications for Acetone. The possible incidence on the chemistry of the upper troposphere motivated us to focus on the adsorption of acetone on transparent ice films doped with nitric acid.

Even if our experimental ice films might be far, in term of ice surface quality, from the real ice crystals existing in the clouds of the upper troposphere (UT), we have estimated the potential impact of nitric acid in ice on the partitioning of acetone in the UT, according to our experimental results.

In the gas-phase, as mentioned previously, the photolysis of acetone is its main loss process in the UT and contributes to form HO_X radicals and PAN.[12] Accordingly, the photochemical lifetime of acetone in the UT is about 20 days.[12] Our experimental results can be used to evaluate the partitioning of acetone between the gas phase and the ice crystals of clouds in the UT, as long as the temperature remains higher than 213 K.

The amount of acetone scavenged by a cirrus cloud can be estimated by assuming that the surface area densities of ice range between 1×10^{-4} and 1×10^{-7} cm^2 cm^{-3}.[5] In the most favorable case, i.e., $[HNO_3] = 1$ N, $T = 213$ K, and an acetone gas-phase concentration of 3 ppbv, which corresponds to 3.4×10^{10} molecules cm^{-3} at a total pressure of ~ 0.3 atm, the surface coverage derived from our results (Figure 3) would be approximately 2×10^{13} molecules cm^{-2}. The number of gas-phase acetone molecules that could be scavenged, is then between 2×10^6 and 2×10^9 molecules cm^{-3}. This corresponds-to-a ratio of acetone molecules adsorbed on the ice surfaces to the number of molecules in the gas phase of $6 \times$

$10^{-5} - 6 \times 10^{-2}$ depending on the ice surface areas in the upper troposphere. This tends to prove that, even in the densest ice clouds, less than 6% of acetone molecules are adsorbed on ice.

The photolysis of adsorbed acetone on ice or its reaction with others adsorbed pollutants will then represent only two minor contributions for its atmospheric fate. Consequently, the formation of HO_X from acetone can only be *promoted* by its photolysis in the gas phase.

Acknowledgment. This work was supported by the EC (Project CUT-ICE, EVK2-CT1999-00005) and by the French Ministry of Research through the PNCA program. This is the EOST contribution No. 2005.104-UMR7517.

References and Notes

(1) Arnold, F.; Bürger, V.; Droste-Fanke, B.; Grimm, F.; Krieger, A.; Schneider, J.; Stilp, T. *Geophys. Res. Lett.* **1997**, *24*, 3017.

(2) Singh, H. B.; Ohara, D.; Herlth, D.; Sachse, W.; Blake, D. R.; Bradshaw, J. D.; Kanakidou, M.; Crutzen, P. J. *J. Geophys. Res.* **1994**, *99*, 1805.

(3) Singh, H.; Chen, Y.; Tabazadeh, A.; Fukui, Y.; Bey, I.; Yantosca, R.; Jacob, D.; Arnold, F.; Wohlfrom, K.; Atlas, E.; Flocke, F.; Blake, D.; Heikes, B.; Snow, J.; Talbot, R.; Gregory, G.; Sachse, G.; Vay, S.; Kondo, Y. *J. Geophys. Res.* **2000**, *105*, 3 795.

(4) Mari, C.; Saüt, C.; Jacob, D.; Ravetta, F.; Anderson, B.; Avery, M. A.; Blake, D. R.; Brune, W. H.; Faloona, I.; Gregory, G. L.; Heikes, B. G.; Sachse, G. W.; Sandholm, S. T.; Singh, H. B.; Talbot, R. W.; Tan, D.; Vay, S. *J. Geophys. Res.* **2003**, *108-D2*, 8229.

(5) Solomon, S.; Borrmann, S.; Garcia, R. R.; Portmann, R.; Thomason, L.; Poole, L. R.; Wnker, D.; McCormick, M. P. *J. Geophys. Res.* **1997**, *102*, 21411−21429.

(6) Winkler, D. M.; Trepte, C. E. *Geophys. Res. Lett.* **1998**, *25*, 3351.

(7) Heymsfield, A. J.; Sabin, R. M. *J. Atmos. Sci.* **1989**, *46*, 2252.

(8) Jacob, D. J.; Field, B. D.; Jin, E. M.; Bey, I.; Li, Q.; logan, J. A.; Yantosca, R. M. *J. Geophys. Res.* **2002**, *107*, 10.1029/2001JD000694.

(9) Holzinger, R.; Warnke, C.; Hansel, A.; Jordan, A.; Lindinger, W. *Geophys. Res. Lett.* **1999**, *26*, 1161.

(10) Warneke, C.; Karl, T.; Judmaier, H.; Hansel, A.; Jordan, A.; Lindinger, W.; Crutzen, P. *J. Global Biochem. Cycles* **1999**, *13*, 9.

(11) Atkinson, R. *Atmos. Environ.* **2000**, *34*, 2063.

(12) Gierczak, T.; Burkholder, J. B.; Bauerle, S.; Ravishankara, A. R. *Chem. Phys.* **1998**, *231*, 229.

(13) Abbatt, J. P. D. *Chem. Rev.* **2003**, *103*, 4783.

(14) Schaff, J. E.; Roberts, J. T. *Langmuir* **1998**, *14*, 1478.

(15) Sokolov, O.; Abbatt, J. P. D. *J. Phys. Chem. A* **2002**, *106*, 775.

(16) Winkler, A. K.; Holmes, N. S.; Crowley, J. N. *Phys. Chem. Chem. Phys.* **2002**, *4*, 5270.

(17) Hudson, P. K.; Zondlo, M. A.; Tolbert, M. A. *J. Phys. Chem. A* **2002**, *106*, 2882.

(18) Peybernès, N.; Marchand, C.; Le Calvé, S.; Mirabel, P. *Phys. Chem. Chem. Phys.* **2004**, *6*, 1277.

(19) Picaud, S.; Hoang, P. N. N. *J. Chem. Phys.* **2000**, *112*, 9898.

(20) Marinelli, F.; Allouche, A. *Chem. Phys.* **2002**, *272*, 137.

(21) Abbatt, J. P. D. *Geophys. Res. Lett.* **1997**, *24*, 1479.

(22) Zondlo, M. A.; Barone, S.; Tolbert, M. A. *Geophys. Res. Lett.* **1997**, *24*, 1391.

(23) Taylor, G. *Proc. R. Soc., London* **1953**, *219*, 186.

(24) Gregg, S. J.; Sing, K. S. W. *Adsorption, Surface Area and Porosity*, 2nd ed.; Academic Press Inc.: San Diego, CA, 1982.

(25) NIST. www.webbook.nist.gov/chemistry.

(26) Petrenko, V. F.; Whitworth, R. W. *Physics of Ice*; Oxford University Press: Oxford, England, 1999.

(27) Peybernès, N.; Le Calvé, S.; Mirabel, P. *J. Chem. Phys. B* **2004**, *108*, 17425.

(28) Picaud, S.; Hoang, P. N. N.; Peybernès, N.; Le Calvé, S.; Mirabel, P. *J. Chem. Phys.* **2005**, *122*, 194707-1.

(29) Beyer, K. D.; Hansen, A. R. *J. Phys. Chem. A.* **2002**, *106*, 10275.

(30) Guimbaud, C.; Bartels-Rausch, T.; Ammann, M. *Int. J. Mass Spectrom.* **2003**, *226*, 279.

(31) Dominé, F.; Rey-Hanot, L. *Geophys. Res. Lett.* **2002**, *29*, 1873.